Key Points:
- Combined analysis of seismic reflection and potential field data reveal a W-E oriented basin system in the NE Norwegian Barents Sea including the Olga and Sørkapp Basins
- Local potential field maxima delineate the Olga and Sørkapp Basins and indicate deep crustal heterogeneities
- Both basins evolved as half-grabens and are underlain by Timanian basement that controlled the later subsidence evolution

Supporting Information:
- Supporting Information S1

Correspondence to:
P. Klitzke,
peter.klitzke@bgr.de

The Paleozoic Evolution of the Olga Basin Region, Northern Barents Sea: A Link to the Timanian Orogeny

P. Klitzke[1] [iD], D. Franke[1] [iD], A. Ehrhardt[1] [iD], R. Lutz[1], L. Reinhardt[1] [iD], I. Heyde[1], and J. I. Faleide[2,3] [iD]

[1]Federal Institute for Geosciences and Natural Resources (BGR), Hannover, Germany, [2]Research Centre for Arctic Petroleum Exploration (ARCEx), UiT - The Arctic University of Norway, Tromsø, Norway, [3]Department of Geosciences, University of Oslo, Oslo, Norway

Abstract The evolution of the Olga Basin region in the northern Norwegian Barents Sea and its relation to the Caledonian and Timanian orogenies is poorly understood due to sparse geophysical data and the lack of well control. In 2015, the German Federal Institute for Geosciences and Natural Resources (BGR) acquired deep multichannel seismic lines as well as gravity and magnetic data. The new seismic data reveal that the Olga and Sørkapp Basins evolved as a W-E striking half-graben system along a major normal fault in the north and a smaller normal fault in the south, respectively. Deep crustal undulating high-amplitude reflections below the Olga and Sørkapp Basins coincide with W-E striking local magnetic maxima and may imply that the basins evolved on top of old collisional fabrics. The absence of major compressional deformation implies a post-Caledonian onset of subsidence. The W-E structural configuration of the sedimentary basins is difficult to reconcile with an earlier proposed NE striking Caledonian branch in the northern Barents Sea. Instead, the orientation of the Olga and Sørkapp Basins lines up with Timanian structural trends from the Pechora Basin. We propose that the Olga and Sørkapp Basins experienced transtensional deformation during the late Devonian/early Carboniferous NE-SW regional extension phase whereby inherited Timanian lineaments controlled the final W-E basin configuration. A salient pre-Caledonian Olga-Sørkapp crustal block in the central Barents Sea would also explain the recently proposed NNW rotation of Caledonian nappes and thrust sheets in the southwestern Barents Sea.

1. Introduction

Research in the Norwegian Barents Sea mainly focused on the petroliferous southwestern Barents Sea and the Svalbard archipelago in the last decades. Accordingly, tectonic concepts of the Barents Sea are predominantly based on information from these regions and sparse data from the Russian Barents Sea, including the archipelagos of Franz Josef Land and Novaya Zemlya.

Little is known about the Norwegian NE Barents Sea including the Olga Basin region. Early studies suggest a late Mesozoic origin for the Olga Basin due to significant thinning or even absence of Cretaceous strata on the bounding Storbanken and Sentralbanken Highs (Figure 1; Antonsen et al., 1991; NPD, 2017). More recent studies support a Cretaceous subsidence phase and speculate about a possible underlying Carboniferous depocenter (Anell et al., 2016). The correlation of positive potential field anomalies with the basin center was explained by a Paleozoic rift system and corresponding intrusives (Grogan et al. 2000). Wide-angle seismic lines reveal crustal heterogeneities that are interpreted as accreted island arcs or oceanic terrains emplaced in the course of the Caledonian collision of Baltica, Laurentia, and the microcontinent Barentsia (Aarseth et al., 2017; Breivik et al., 2002). However, the relationship between the evolution of W-E striking Olga Basin and the underlying basement grain remains only poorly understood (Figure 1).

Newly acquired multichannel seismic by the German Federal Institute for Geosciences and Natural Resources (BGR) for the wider Olga Basin region allow an unprecedented detailed view into the Paleozoic evolution of the NE Norwegian Barents Sea. The combined interpretation of seismic and potential field data allows us to investigate the structural configuration of the Olga Basin and discuss its evolution with regard to inherited structures and in light of existing tectonic models.
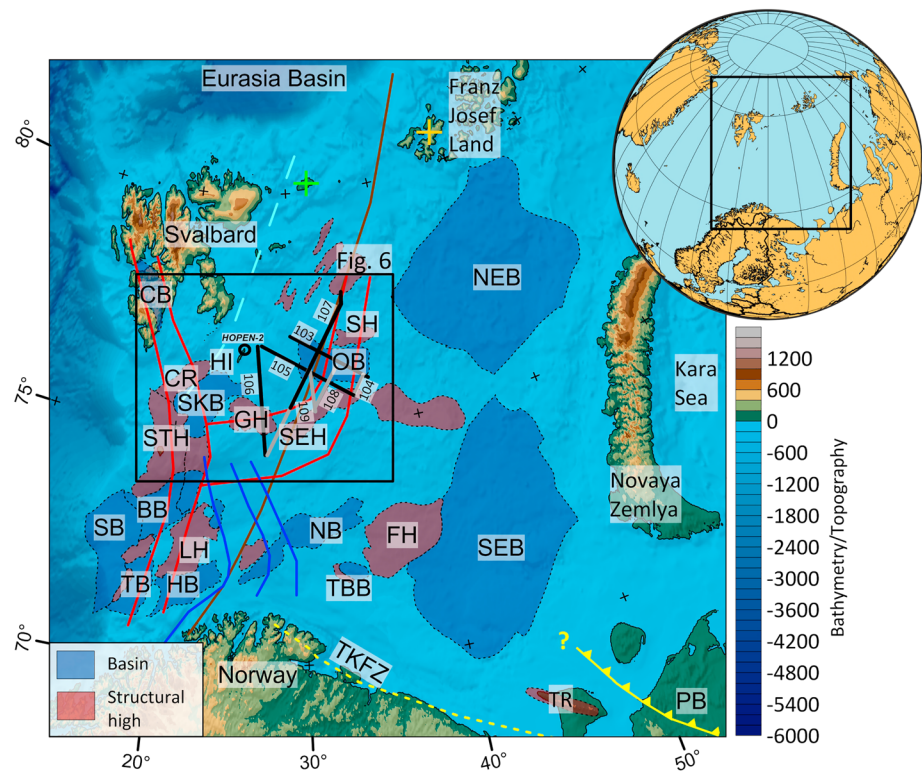
Figure 1. Major offshore structures in the Barents Sea. The black lines show the location of seismic data from the BGR-2015 survey shown in Figures 2–5. The colored lines show published Caledonian trends. The red and brown lines indicate two branches (brown (Gee et al., 2006) and red (Aarseth et al., 2017)). Other proposed Caledonian structures are light blue (Barrère et al., 2011), dark blue (Gernigon et al., 2014), and green cross (Gee & Pease, 2004). Timanian trends are delineated by yellow lines (Gee et al., 2006) and a yellow cross (Franz-Josef Land; Pease, 2011). The red and blue polygons outline structural highs and basinal areas. BB = Bjørnøya Basin, CB = Central Tertiary Basin, CR = Capria Ridge, FH = Fedinsky High, GH = Gardabanken High, HB = Hammerfest Basin, HI = Hopen Island, LH = Loppa High, NB = Nordkapp Basin, NEB = NE Barents Sea Basin, OB = Olga Basin, PB = Pechora Basin, SEB = SE Barents Sea Basin, SEH = Sentralbanken High, SH = Storbanken High, SKB = Sørkapp Basin, SB = Sørvestnaget Basin, STH = Stappen High, TB = Tromsø Basin, TBB = Tiddlybanken Basin, TKFZ = Trollfjorden-Komagelva Fault Zone, TR = Timan Range.

2. Geological Setting

2.1. Basement Grain

It is generally accepted that the basement of the wider Barents Sea region was assembled during the Timanian (Precambrian-Cambrian), Caledonian (Silurian-Devonian), and Uralian (Carboniferous-Permian, mid-Jurassic) orogenies (Estrada et al., 2018; Gee et al., 2006, 2008; Gee & Pease, 2004; Gudlaugsson et al., 1998; Knudsen et al., 2017; Pease, 2011; Ritzmann & Faleide, 2007). The Precambrian-Cambrian Timanian orogeny evolved as fold-and-thrust belt along the NE margin of Baltica (Gee et al., 2006, 2008; Gee & Pease, 2004). Evidence of the Timanian orogeny is the Trollfjorden-Komagelva Fault Zone (yellow dashed line in Figure 1) that extends from the polar Urals across the Timan Range as far as to the Varanger peninsula in northern Norway, where the structures are reworked by younger Caledonian trends (Gernigon et al., 2014; Gernigon & Brönner, 2012). Timanian basement was drilled in the Pechora Basin in Russia and is associated with different basement terranes including accreted Neoproterozoic fragments and metamorphosed sedimentary, volcanic, and volcanoclastic rocks (Figure 1; Dovzhikova et al., 2004; Roberts & Siedlecka, 2002). These trends are well described onshore and delineated offshore by characteristic potential field anomalies that extend into the Pechora Sea (yellow dotted line in Figure 1). The NW-SE orientation of the Tiddlybanken Basin south of the Fedinsky High is a further indication for the presence of Timanian basement in the SE Barents Sea (Gernigon et al., 2018). Detrital zircon dating from northern Taymir and a Cambro-Ordovician unconformity on Severnaya Zemlya (east of Franz-Josef Land) imply that the Timanides extended northward across the entire eastern Barents Sea as far as

to the northern Kara Sea (Gee et al., 2006, 2008; Pease, 2011). This is supported by similar magnetic intensity patterns in the Pechora Basin and in the northern Kara Sea (Gee et al., 2006), which are likely obscured in the eastern Barents Sea by sediment thicknesses of up to 20 km (Faleide et al., 2018; Ivanova et al., 2011; Klitzke et al., 2015, 2016).

Two end-member models are discussed for the Caledonian orogeny—a "one-branch suture" and a "bifurcating suture" (Figure 1; Aarseth et al., 2017; Barrère et al., 2009, 2011, Breivik et al., 2002, 2003, 2005; Doré et al., 1997; Faleide et al., 1984; Gabrielsen et al., 1990; Gee et al., 2006, 2008; Gernigon et al., 2014; Gernigon & Brönner, 2012; Gudlaugsson et al., 1998; Henriksen et al., 2011; Marello et al., 2013; Ritzmann & Faleide, 2007, 2009; Worsley, 2008). The "one-branch models" are based on the interpretation of NE-SW oriented Carboniferous rift basins in the SW Barents Sea in prolongation of Caledonian thrusts and nappes of onshore Scandinavia (brown line in Figure 1). This led to the conclusion that these basins evolved on top of a similarly striking Caledonian basement grain in the SW Barents Sea. However, Caledonian migmatization in east Svalbard (green cross in Figure 1; Gee & Pease, 2004; Tebenkov et al., 2002) and Timanian detrital muscovite on Franz-Josef Land (yellow cross in Figure 1; Pease, 2011) suggest a Caledonian suture between the two archipelagos in the northern Barents Sea. The bifurcating model includes an additional N-S oriented branch toward Svalbard parallel to the present-day western Barents continental margin (combined brown and red lines in Figure 1; Breivik et al., 2002; Gudlaugsson et al., 1998). Based on OBS data, the eastern Caledonian suture was proposed to branch off east of Bjørnøya Island (on Stappen High) toward the northeast (Figure 1; Aarseth et al., 2017). The interpretation of this NE oriented Caledonian branch is based on the topography of the basement and the Moho, a westward lateral crustal velocity decrease and crustal reflectivity increase across the Gardabanken High (Aarseth et al., 2017; Breivik et al., 2002, 2003, 2005; Eiken, 1994; Ritzmann & Faleide, 2007).

Recently, these geological models were challenged based on combined interpretation of magnetic and seismic data and a rotation of Caledonian nappes from a SW-NE trend on the Norwegian mainland to a SSE-NNW trend in the SW Barents Sea was proposed (dark blue line in Figure 1; Barrère et al., 2009, 2011; Gernigon et al., 2014; Gernigon & Brönner, 2012). These zones of interpreted Caledonian deformation are narrowing northward and appear to line up with N-S striking Caledonian grain on Bjørnøya and Svalbard (Harland & Wright, 1979; Manby & Lyberis, 1992; Worsley, 2008). Similar magnetic patterns east of Svalbard indicate that the Caledonian collision zone is widening again in the northern Barents Sea (Barrère et al., 2011).

2.2. Geological Evolution and Depositional Regime

The oldest sedimentary basins in the SW Barents Sea apparently follow the SSE-NNW striking trend of the Caledonian nappes and are likely of late Devonian/early Carboniferous age and associated with extensional reactivation of inherited Caledonian structures (Gernigon et al., 2014). Onshore Svalbard and Bjørnøya these basins contain strata of Silurian(?) to Devonian age and obtain cumulative sediment thicknesses of up to 8 km (Dallmann et al., 2015). Devonian to early Carboniferous rifting is also described for the Pechora Basin and the eastern Barents Sea (Stoupakova et al., 2011).

During Early Carboniferous times, a warm and humid climate prevailed that led to deposition of coal beds found at several locations across Svalbard, the Finnmark Platform, and the southern Barents Sea (Faleide et al., 1984; Gudlaugsson et al., 1998). Toward the end of the Early Carboniferous the climate shifted to semi-arid and arid conditions that resulted in a change of the depositional environment to more siliciclastic deposits (Dallmann et al., 2015; Van Koeverden et al., 2010). Caledonian basement trends in the SW Barents Sea were partly reactivated and crosscut by mid-Carboniferous rifting which resulted in a mosaic of horst and graben structures (Gernigon et al., 2014). With the Late Carboniferous global sea level rise graben structures were successively flooded, accompanied by deposition of evaporites. Salt deposits in the, for example, Nordkapp and Tromsø Basins, are imaged by seismic data, supported by gravity and magnetic data, and most likely were mobilized during Triassic times (Breivik et al., 1995; Faleide et al., 1984; Gernigon et al., 2011; Gudlaugsson et al., 1998; Perez-Garcia et al., 2013; Smelror et al., 2009; Stadtler et al., 2014). Horst structures were transgressed during the Late Carboniferous and widespread carbonate platforms developed (Dallmann et al., 2015) until early Permian times. During phases of high sea level the entire shelf was flooded and shallow-water platform carbonates developed on the Finnmark Platform, Loppa High, and Stappen High. In the middle to late Permian, a shift to the deposition of cold water and deepwater fine clastics and

silica-rich spiculites occurred (Worsley, 2008). A major plate reorganization toward the end of the Paleozoic led to the closure of the Uralian seaway and the development of the Uralides which were a major source of clastic sediments into the Barents Sea in Permo-Triassic times (Puchkov, 2009).

Late Permian-Early Triassic rifting is controversially discussed in the western Barents Sea. While some authors claim that the Triassic was a tectonically quiet period, particularly in the northern Barents Sea and Svalbard region (Gabrielsen et al., 1990; Høy & Lundschien, 2011; Klausen, 2013; Pózer Bue & Andresen, 2014; Riis et al., 2008; Worsley, 2008), there is evidence for extensional deformation on Svalbard, in the Bjørnøya Basin, and the Fingerdjupet Subbasin (Anell et al., 2013; Blaich et al., 2017; Osmundsen et al., 2014; Serck et al., 2017). Renewed tectonic activity was apparent toward the middle Jurassic in both the North Atlantic and the Arctic regions, continuing into earliest Cretaceous time involving multiple phases of extension and magmatism (Blaich et al., 2017; Clark et al., 2014; Corfu et al., 2013; Faleide et al., 1993, 2010; Maher, 2001; Polteau et al., 2015; Serck et al., 2017). Episodes of pronounced inversion and erosion affected the Barents shelf region during the late Mesozoic and Cenozoic (Baig et al., 2016; Dimakis et al., 1998; Green & Duddy, 2010; Henriksen et al., 2011; Sobolev, 2012; Zattin et al., 2016).

3. Data Acquisition, Processing, and Velocity Modeling

Geophysical data were acquired by the German Federal Institute for Geosciences and Natural Resources (BGR) during a cruise with research vessel OGS Explora in the frame of the PANORAMA project in late summer 2015. Bathymetric mapping was conducted during the cruise using the ship's Reson SeaBat system. Magnetic data were acquired with a SeaSpy gradient magnetometer system with two scalar Overhauser magnetometers and a vector magnetometer. The gravitational field was measured using a KSS31 gravimeter system. The reflection seismic source was a G gun array with a total volume of 2,000 in^3 (32.8 L; working pressure 14.5 MPa) and a towing depth of 6 m throughout the survey. The regular shot distance was 25 m. A 3,600-m-long, 288-channel Seal streamer towed at a depth of 12 m recorded the data at 2-ms sampling rate. The record length was 9 s. Additionally, we used magnetic and gravity data from the compilations of the Circum-Arctic mapping project (Gaina et al., 2011) and DTU2013 (Andersen et al., 2014) for regional potential field maps. We calculated from the regional magnetic grid the depth to magnetic sources using Source Parameter Imaging (Geosoft). We project the solutions in vicinity on the respective seismic line.

Eight multichannel seismic lines were acquired with a total length of ~1,750 km. Within this study we present the regional profiles BGR2015–103, BGR2015–105, BGR2015–106, and BGR2015–107 (Figures 1, 2, 3, and 4). BGR2015–103 and BGR2015–107 traverse the Olga Basin as defined by the Norwegian Petroleum Directorate (Blystad et al., 1995; Gabrielsen et al., 1990; NPD, 2017) lengthways and perpendicular to the assumed basin axis, respectively. Line BGR2015–105 runs parallel to BGR2015–103 crosscut the southernmost tip of the Olga Basin and terminate on the Sentralbanken High in the east. Line BGR2015–106 is N-S oriented and covers the region east of Hopen Island in the north and the Gardabanken High in the south (Figure 1). For better control on seismic velocities, the MCS method was expanded by sonobuoy wide-angle and refraction measurements.

Due to shallow water conditions (water depth of ~100 to ~500 m) and the highly compacted sediments at the seafloor, the data are strongly biased by multiples. Therefore, the data processing sequence was especially focused on signal enhancement and multiple removal. In order to remove the significant bubble energy from the data we used the recorded source signal from the water break hydrophone as input for the designature operator. For multiple removal two iterations of surface-related multiple elimination were applied to the data. After a first velocity analysis the signal/noise ratio was enhanced with common reflection surface processing, followed by a second velocity analysis. A poststack predictive deconvolution eliminated remaining reverberations. This stack result was Kirchoff-time-migrated using a smoothed migration velocity model.

4. Interpretation

Owing to the lack of deep explorations wells, the age assignment of individual seismic reflectors in multichannel seismic data in the northern Norwegian Barents Sea is tentative. A few shallow stratigraphic drillings from the Sentralbanken High and palynological analysis from the Olga Basin reveal middle Triassic to Early Cretaceous ages for the uppermost consolidated sediments (Antonsen et al., 1991; Lundschien et al., 2014; NPD, 2017; Riis et al., 2008). The only available well that penetrates Upper Paleozoic
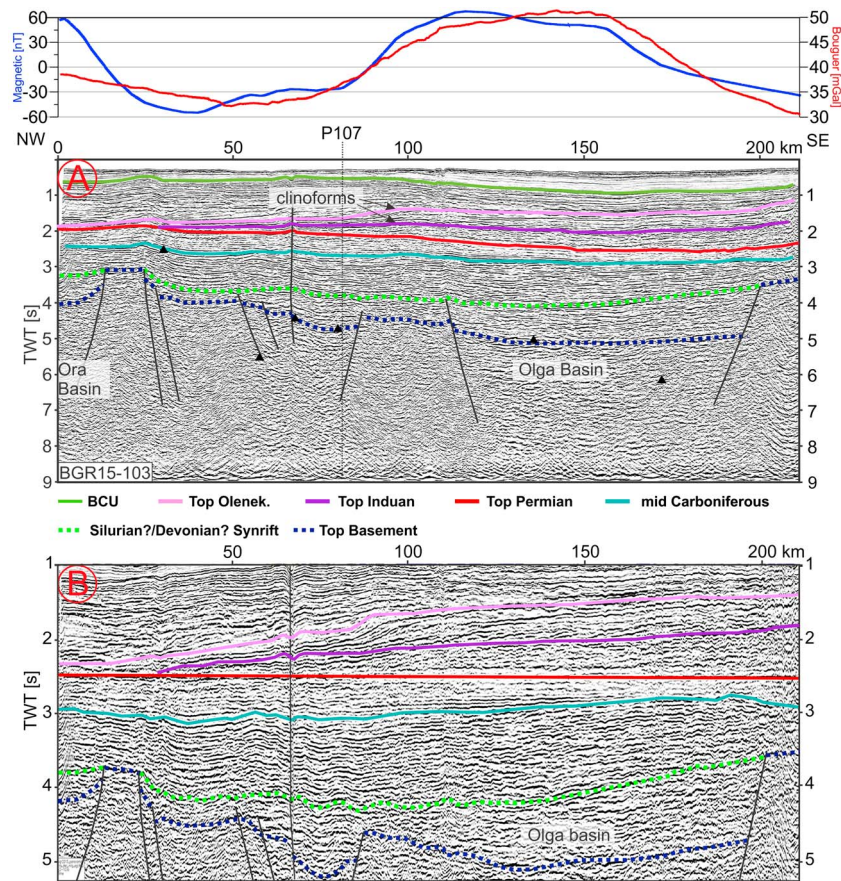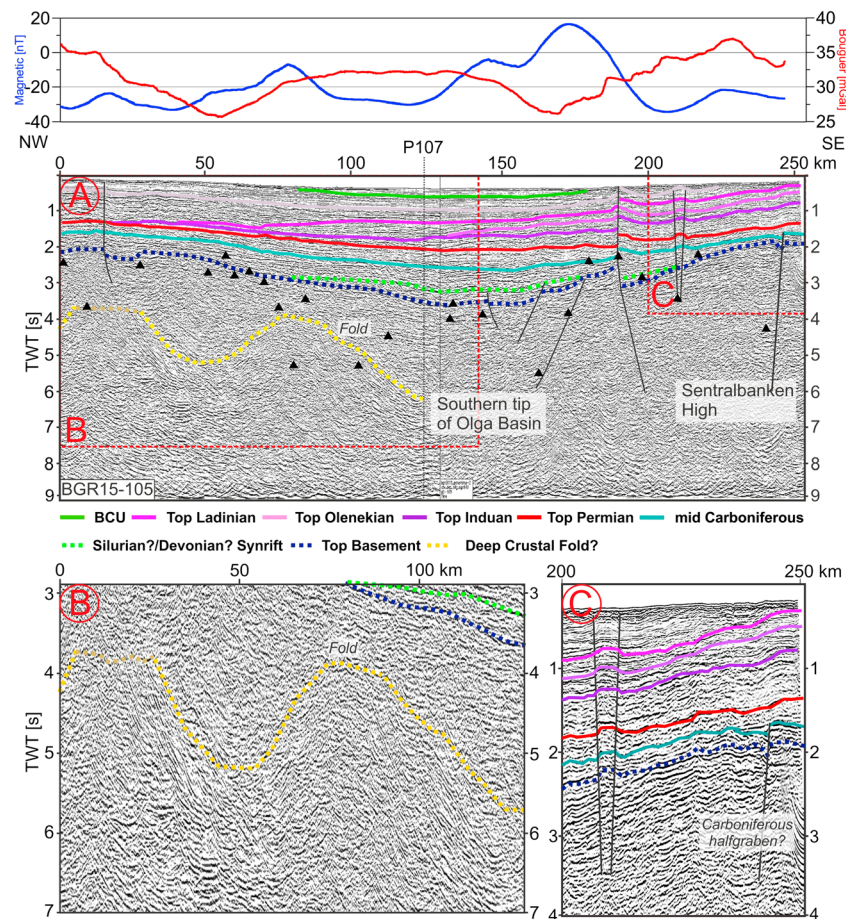
Figure 2. NW-SE striking profile BGR2015–103. See Figure 1 for location. (a) This line reveals fault-controlled initial subsidence. The center of the Olga Basin is accompanied by positive gravity and magnetic anomalies. The Ora Basin in the northwesternmost part of the profile (Anell et al., 2016) is poorly defined. BCU corresponds to the base Cretaceous unconformity. Black triangles indicate the projected depth to magnetic sources. (b) BGR2015–103 flattened on the near-top Permian reflector to illustrate northwestward shifting depocenter in the postextensional phase. During Triassic times regional subsidence dominated and the shelf was infilled with clastic material from the eroding Ural Mountains resulting in the formation of prominent clinoforms. Mild Carboniferous compression is evident between 0 and 75 km. Uninterpreted section is provided in the supporting information.

sediments in the northern Norwegian Barents Sea is Hopen-2 at the northern tip of Hopen Island (Figure 1). Anell et al. (2014, 2016) correlate the Hopen-2 well with multichannel seismic lines that provide the so far best estimates of the likely reflector ages down to mid-Carboniferous strata. In the following, we tie our western reflection seismic lines to their interpretation. Additionally, we make use of published regional seismic profiles that are tied to well data in the southern Barents Sea (e.g., Clark et al., 2014; Glørstad-Clark et al., 2010) to further constrain our interpretation. We consider the interpretation of the base Cretaceous, top Ladinian, top Olenekian, top Induan (Early and Middle Triassic), and top Permian seismic horizons as quite robust, and a mid-Carboniferous seismic horizon as fair. Accordingly, we describe the interpretation of the sedimentary column from top downward, beginning with the highest confidence level.

4.1. Mesozoic Succession

Multiple episodes of pronounced Cenozoic inversion, uplift, and glaciations resulted in removal of most of the Cenozoic and upper Mesozoic sediments (Dimakis et al., 1998; Henriksen, Bjørnseth, et al., 2011; Rasmussen & Fjeldskaar, 1996; Sobolev, 2012).

Palynological analyses reveal a Cretaceous age for the uppermost consolidated sediments of the Olga Basin (Antonsen et al., 1991). The base Cretaceous is correlated with the Berriasian hiatus causing a strong
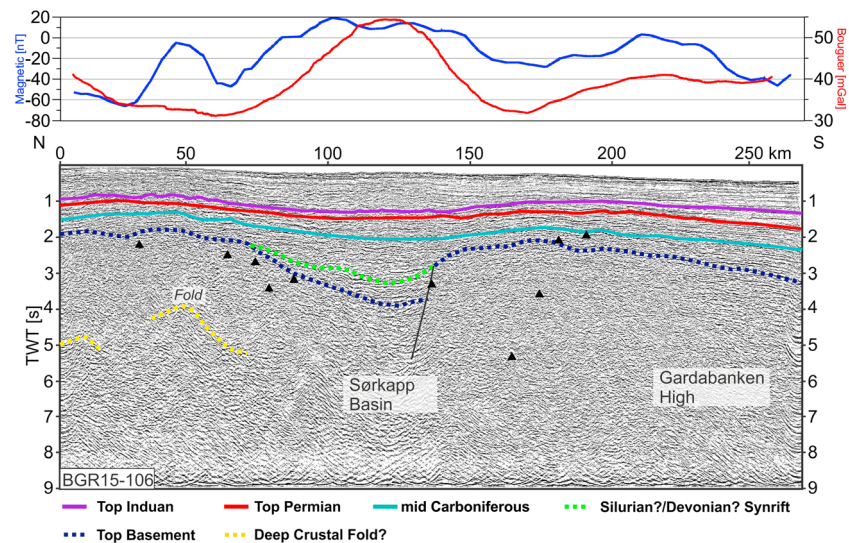
Figure 3. (a) NW-SE striking profile BGR2015–105 traverses the southern tip of the Olga Basin. Black triangles indicate the projected depth to magnetic sources. See Figure 1 for location. (b) Enlargement showing the interpreted deep crustal folds in the northern part of the line. (c) Zoom to the south of BGR2015–105. Enlargement showing the deep basement faults that were likely reactivated in late Mesozoic-early Cenozoic times. Uninterpreted section is provided in the supporting information.

impedance contrast and prominent reflectivity (Figures 2, 3, and 5; Antonsen et al., 1991; Grundvåg et al., 2017). The corresponding Cretaceous layer has a maximum thicknesses of 0.5 s TWT in the Olga Basin, and thins northward on the Kong Karl Platform (0.2 s TWT), while it pinches out toward the south on the flanks of the Sentralbanken High (Figures 2 and 5). The presence of Jurassic strata within the Olga Basin is uncertain. Jurassic sedimentation is associated with major eustatic sea level changes that led to a generally high condensation of deposits. Prominent reflections can indeed be found below the Cretaceous strata in the seismic profiles which may indicate the presence of a condensed Jurassic succession.

Triassic strata are confirmed by shallow stratigraphic boreholes on the Sentralbanken High, south of the Olga Basin (Lundschien et al., 2014; Riis et al., 2008). These wells guided shallow seismic interpretations in this region and allow us to tie our reflection data to published seismic lines (Høy & Lundschien, 2011; Lundschien et al., 2014; NPD, 2017; Riis et al., 2008). During Triassic times sediments were deposited in a distinctly prograding siliciclastic shelf margin system. Major clinoforms are well described from seismic studies and allow us to decipher the Lower Triassic strata that are not penetrated by stratigraphic boreholes (Høy & Lundschien, 2011; Lundschien et al., 2014; NPD, 2017; Riis et al., 2008).

The Early to Middle Triassic in the Barents Sea was dominated by prograding transgressive-regressive sequences (Glørstad-Clark et al., 2011). Our seismic data image several prominent reflectors that bound two major sets of clinoforms belts of different age. The oldest clinoform belt is interpreted to be of Induan age and downlaps on Permian spiculites (Figures 2 and 5). Subsidence around Induan-Olenekian times resulted in a major transgression and the generation of further accommodation space. As a consequence
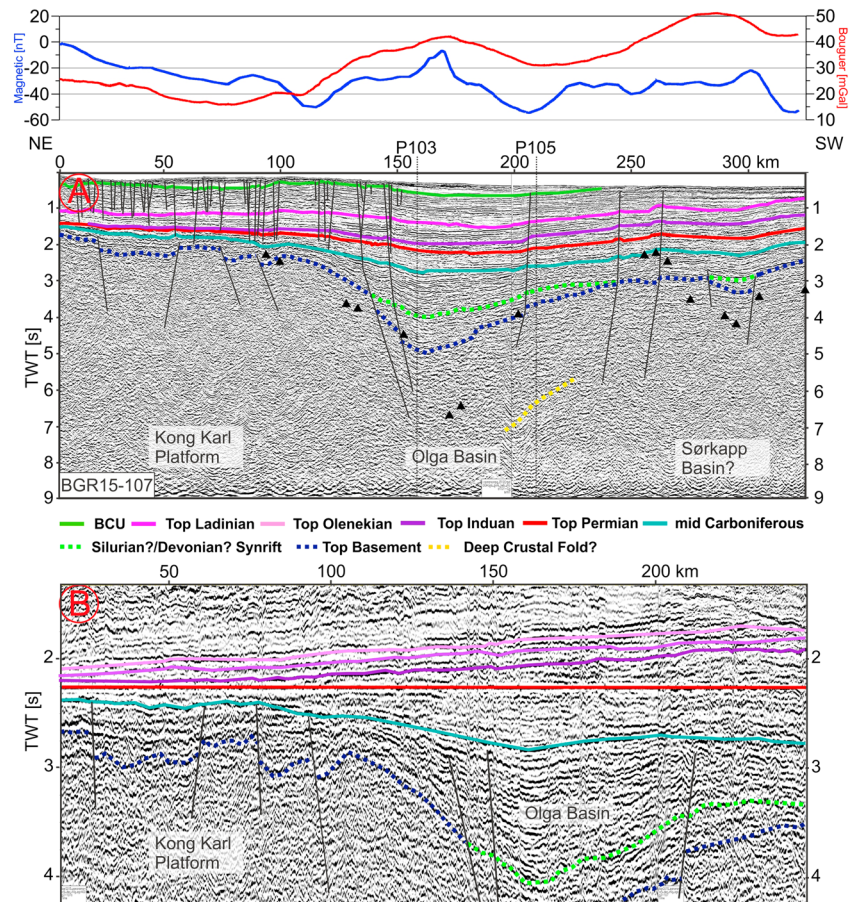
Figure 4. N-S striking profile BGR2015–106. See Figure 1 for location. Steep normal faults bound a deep basin that represents the eastern extension of the Sørkapp Basin. The eastern Sørkapp Basin is a half-graben with the major basin-bounding fault in the south. A wedge-shaped sedimentary succession filling the half-graben indicates syn-extensional deposition. Black triangles indicate the projected depth to magnetic sources. Minor folded metasediments are distinct in the northern portion of the line. Similar to the Olga Basin, the Sørkapp Basin depocenter is accompanied by positive gravity and magnetic anomalies. Uninterpreted section is provided in the supporting information.

the progradation temporarily ceased and the Olenekian clinoform belt evolved further landward on top of the Induan clinoforms (Figure 2). The overlying Ladinian clinoform belt prograded further westward, indicating that regional subsidence slowed down again. The long transportation distance of clastic material from the Urals likely led to the deposition of predominantly mudstone-rich fine-grained sediments with poor reservoir quality (Eide et al., 2017). Several highs such as the Gardabanken High, the Capria Ridge, and Hopen High are assumed to have experienced flexural uplift during Triassic times (Anell et al., 2016). Upper Triassic sediments reveal no clear clinoforms and indicate that the southeastern sediment source ceased and another source from Greenland, Taimyr, and Severnaya Zemlya provided additional sediments (Fleming et al., 2016). Triassic deposits constitute the largest portion of the Mesozoic succession in our data with an average thickness of ~1.75 s TWT (Figures 2, 3, and 5). Toward the north, the sediments are thinning slightly across the Kong Karl Platform (~1.4 s TWT; Figure 5). South of the Olga Basin, the uppermost Triassic sediments are eroded on the Gardabanken and Sentralbanken Highs (Figures 3 and 5).

4.2. Paleozoic Succession

Two prominent reflection bands in our seismic data are distinctively similar to deep reflections in several seismic surveys across wide parts of the Norwegian Barents Sea (Figures 2–5; Anell et al., 2014, 2016; Blaich et al., 2017; Breivik et al., 1995; Faleide et al., 1984; Gudlaugsson et al., 1998; Koehl et al., 2018; NPD, 2017). During the end of the Permian, widely deposited and strongly cemented spiculitic shales became rapidly draped by shales and sandstones. The drastic lithological change results in a major impedance contrast, marking the end of the Permian in the Barents Sea (Anell et al., 2014, 2016; Glørstad-Clark et al., 2010; Gudlaugsson et al., 1998; Koehl et al., 2018). Thus, we assign a near-top Permian age to the upper Paleozoic reflection. The second prominent reflection is suggested to be associated with the mid-Carboniferous sea level rise, corresponding transgression and the lithological change from sandstones and shales to silicified deposits, carbonates, and evaporites (Gérard & Buhrig, 1990; Larssen et al., 2002; Worsley et al., 2001). This interpretation is well in line with results from the Hopen-2 well, where Anell et al. (2014) found similar reflection bands to coincide with two major lithological changes representing the end of Permian and the mid-Carboniferous.

The interpreted mid-Carboniferous to Permian sediments are thickest in the Olga Basin (0.5 s TWT), but exhibit only a minor thickness decrease toward the south (0.4 s TWT; Figures 3a and 5b). In the north,

Figure 5. (a) The NE-SW striking profile BGR2015–107 reveals fault-controlled initial subsidence. Syn-extensional infill is indicated by the wedge-shaped strata. The center of the Olga Basin is accompanied by positive gravity and magnetic anomalies. Black triangles indicate the projected depth to magnetic sources. The calculated solutions were projected on the profile. See Figure 1 for location. (b) BGR2015–107 flattened on the near-top Permian reflector. Subsidence was generally lower across the Kong Karl Platform in the north. During Permian times regional subsidence dominated and the shelf was infilled with clastic material from the eroding Ural Mountains resulting in the formation of prominent clinoforms. Uninterpreted section is provided in the supporting information. See Figure 1 for location.

these sediments are significantly thinner across the Kong Karl Platform (0.1 s TWT). Within the Olga Basin, sedimentation was more pronounced in the western part of the basin (Figure 2b). The absence of intense mid-Carboniferous faulting of the Olga Basin region is in sharp contrast to the evolution of the southern and western Barents Sea. Widespread mid-Carboniferous rifting resulted in subsidence of the Nordkapp and Hammerfest Basins and initiated the Fingerdjupet Subbasin and Bjørnøya Basin (Anell et al., 2014, 2016). Some of these basins were filled with extensive salt deposits that were mobilized in Triassic times due to differential loading or thin-skin extension (Breivik et al., 1995; Faleide et al., 1984; Gudlaugsson et al., 1998; Nilsen et al., 1995; Perez-Garcia et al., 2013; Stadtler et al., 2014). A small NE-SW striking half-graben is interpreted below the Sentralbanken High in the easternmost part of profile BGR2015–105 (Figure 3) as also mapped by the NPD (2017). This implies that Carboniferous proto-Atlantic rifting and basin formation extended far to the northeast (NPD, 2017), although the corresponding basins decrease in size. However, we find no indications for evaporites and salt tectonics within the Olga Basin as evident in the Nordkapp and Tiddlybanken Basins and across the Kong Karl Platform (Nilsen et al., 1995; NPD, 2017; Stadtler et al., 2014).

Notably, the newly acquired seismic data reveal horizontally parallel layered reflections below the inferred mid-Carboniferous horizon, implying a sedimentary origin. These sediments are at depths of 3–5 s TWT and are structurally differentiated into two parts. The wedge shape of the lower portion of the sediments indicates a syn-extensional origin bounded by a major normal fault. The syn-extensional succession attains
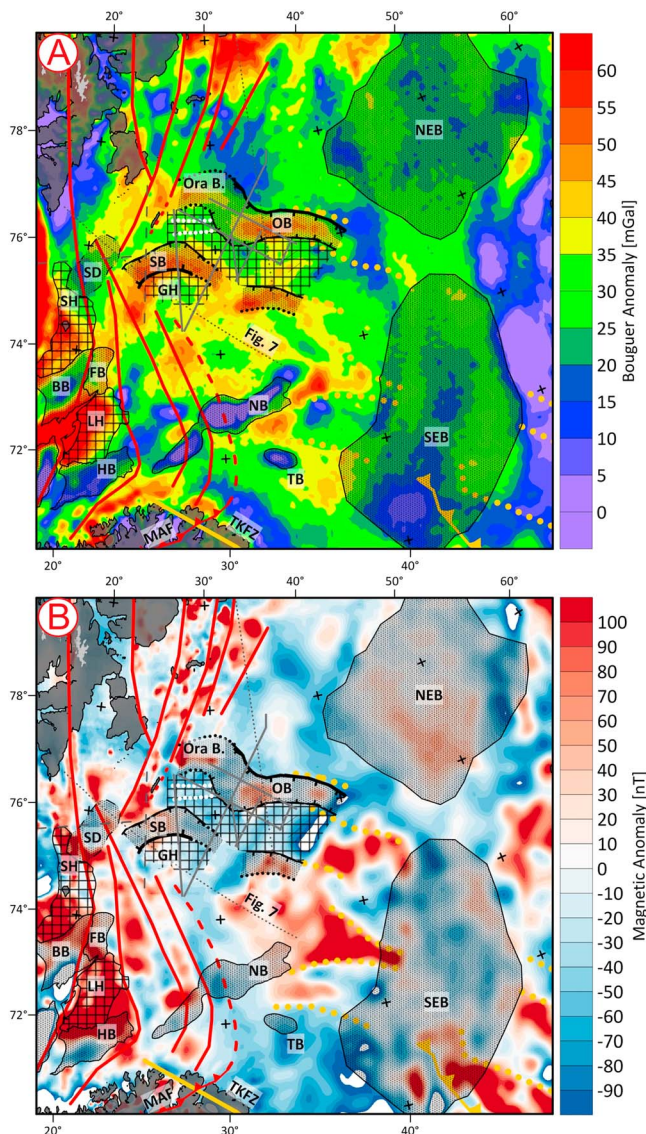
Figure 6. Extent of the Ora/Olga (OB) and Sørkapp Basins (SB) superimposed on (a) gravity and (b) magnetic data with the interpreted prolongation of Timanian structures (yellow) into the central Barents Sea. The outline of the Olga and Sørkapp Basins is delineated by solid black lines (where covered by data and dotted where inferred). Red lines = Caledonian collision zone based on Barrère et al. (2011) and Gernigon et al. (2014). Dotted white line = assumed fold axis. Gray lines = acquired multichannel seismic profiles. Dotted gray line = published data (Breivik et al., 2003, 2005; Glørstad-Clark et al., 2010; Høy & Lundschien, 2011; NPD, 2017). BB = Bjørnøya Basin, FB = Fingerdjupet Subbasin, GH = Gardabanken High, HB = Hammerfest Basin, LH = Loppa High, MAF = Middle Allochthon Front, NB = Nordkapp Basin, NEB = NE Barents Sea Basin, SD = Sørkapp Depression, SEB = SE Barents Sea Basin, SEH = Sentralbanken High, SH = Stappen High, TB = Tiddlybanken Basin, TKFZ = Trollfjorden-Komagelva Fault Zone.

thicknesses locally up to 1 s TWT. The upper sedimentary succession was deposited over a much wider area than the syn-extensional sediments. The overlying sediments are thickest in the Olga Basin (1.5 s TWT) and thin significantly northward across the Kong Karl Platform (0.25 s TWT) and toward the south (0.75 s TWT; Figure 5). This succession has not been affected by significant faulting and thus appears to resemble a postrift thermal sag phase.

The underlying basement cannot be interpreted with confidence. Therefore, we mapped the deepest continuous parallel reflections, displaying the oldest sediments overlying the acoustic basement. Additionally, we calculated the depth to magnetic sources using the Source Parameter Imaging tool on base of the regional magnetic field. Projecting the Source Parameter Imaging solutions on the seismic lines reveals that the seismically interpreted acoustic basement coincides in most parts with the depth to magnetic sources (Figures 2–6).

Distinct normal faults at the rims of the Olga Basin (Figures 2, 3, and 5) show that fault activity was clearly more severe in the north so that the Olga Basin evolved mainly as half-graben (Figure 5). The basin-parallel profile BGR2015–103 displays a gentle southeastward deepening of the Olga Basin. A horst structure forms the NW limit of the Olga Basin (Figure 2). Additionally to the major basin-bounding faults, the W-E profile illustrates minor deformation throughout the basin that may indicate some obliquity during basin initiation. Another basin, the Ora Basin, is proposed west of the horst structure at the NW limit of the Olga Basin (Anell et al., 2016), but is only poorly visible in line BGR2015–103.

5. Basin Structure and Architecture

5.1. Olga Basin

The onset of basin formation is difficult to assess on the basis of the vague Paleozoic stratigraphy. An upper limit for the onset of extensional deformation in the Olga Basin is here proposed to be the Caledonian orogeny. Caledonian deformation was found across wide parts of the northern Norwegian Barents Sea and reached as far as Franz-Josef Land and Severnaya Zemlya in the east and, thus, should have affected also the Olga Basin region. However, in our data there is no indication of major postdepositional compressional deformation affecting the wedge-shaped syn-extensional sediments. The basin thus most likely was initiated following the Caledonian orogeny. Subsidence shifted northwestward with time as indicated by thickening of Late Carboniferous to near-top Permian deposits (Figure 2b).

The new seismic data clearly resolve the half-graben development of the Olga Basin following extension along a W-E striking normal fault bounding the basin in the north. The deepest mapped structures are undulating deep crustal high-amplitude reflections at depths of 3.5–6 s TWT with a wavelength of 50 km (Figure 3: BGR2015–105, 0–100 km and Figure 4: BGR2015–106, 30–70 km; supporting information). These reflections are surrounded by rather chaotic reflection patterns indicating crystalline basement. Although continuous mapping of the high-amplitude reflections across the entire study area is not possible, their presence across the intersecting profiles 105 and 107 supports the robustness of the data (yellow lines in Figures 3 and 5). We interpret these undulating reflections as folds. Their topography correlates well with local magnetic maxima visible in the acquired 2-D magnetic data (Figures 3 and 4) as well as in the compiled regional magnetic map (Figure 6b). A W-E

oriented local magnetic maximum links the top of the two most prominent anticlines on BGR2015–106 and BGR2015–105 and lines up with the axis of the Olga Basin (white stippled line in Figure 6b). Similar parallel reflections in the deeper crust are typically found in orogenic settings (Franke et al., 2008; Koehl et al., 2018) and indicate that the Olga Basin may have evolved above old W-E striking collisional fabrics.

The W-E trend is further supported by distinct positive gravity (+40 mGal) and magnetic anomalies (+80 nT) across the center of the Olga Basin. This correlation allows further mapping of the Olga Basin beyond the seismic data. Pronounced local gravity maxima indicate that the Olga Basin extends further east than previously defined by the Norwegian Petroleum Directorate (NPD, 2017; Figure 6a). Toward the west, the Ora Basin (Anell et al., 2016) is situated in prolongation of the Olga Basin and similarly characterized by positive potential field anomalies (Figure 6). BGR2015–103 illustrates that the Ora and Olga Basins are separated by a horst structure and a local gravity minimum, but may be part of the same graben system (Figures 2 and 6). West of the Ora Basin, the trends of the positive potential field anomalies are truncated by short-wavelength NE striking anomalies crossing the Kong Karl Platform (Figure 6b).

The similar basin-scale wavelength of the gravity and magnetic anomalies implies a similar source below the Olga Basin. The poor correlation of the potential field anomalies with the topography of the acoustic basement mapped here and the Moho imaged by ocean bottom seismometers (Breivik et al., 2002) suggest an intracrustal heterogeneity. In theory, a basin-wide anomaly can be caused by a broad shallow or a narrow deep source. The presence of dolerites onshore northern Norway and on Svalbard proves several magmatic phases from late Precambrian to Cretaceous times which may have affected also the Olga Basin. Most prominent are widespread Cretaceous dolerites sampled onshore Svalbard and Franz-Josef Land (Maher, 2001). Corresponding sills and dikes are also interpreted offshore in the northern Barents Sea (Minakov et al., 2012, 2017). Polteau et al. (2015) recently proposed the presence of shallow igneous sheet intrusions also in the Olga Basin region. We find no evidence for shallow intrusions or sills in our seismic data, which may indicate a deeper crustal source causing the gravity and magnetic anomalies. Interestingly, late Cretaceous and Cenozoic inversion is mostly restricted to the Kong Karl Platform in the north and to the Sentralbanken High in the south of the Olga Basin which may favor the idea of an underlying rigid crustal block.

5.2. Relationship to the Sørkapp Basin

Deep parallel reflections below the mid-Carboniferous horizon at depths of 3–4 s TWT (Figure 4) indicate a so far unknown half-graben to the southwest of the Olga Basin. Interestingly, this graben shares a number of structural similarities with the Olga Basin. A syn-extensional phase is also characterized by wedge-shaped sediments attaining thicknesses of up to 1 s TWT which are bounded by a normal fault in the south. The basin center also coincides with positive potential field anomalies (Figure 4). The combined analysis of published seismic lines and the gravity field illustrates that the half-graben forms the structural link between two Paleozoic basins. Anell et al. (2014, 2016) mapped an eastward prolongation of the Sørkapp Basin terminating west of line BGR2015–106 and another poorly imaged Paleozoic basin to the east. BGR2015–106 fills the spatial gap and suggests that the Sørkapp Basin extends even further east. Unlike Anell et al. (2016) we find no evidence that this basin stretches as far as to the Olga Basin, but that it appears to continue further south on line BGR2015–107 although it clearly decreases in size (Figures 5 and 6).

Toward the west, we propose a redefinition of the conventionally understood N-S oriented Sørkapp Basin (Gabrielsen et al., 1990). A seismic line published by Glørstad-Clark et al., 2010 (Figure 7) illustrates that the western part of the Sørkapp Basin is characterized by a shallower Paleozoic half-graben system that follows the underlying Caledonian basement grain. This western part was partly reactivated in Mesozoic times and informally named the Sørkapp Depression by Anell et al. (2014). The eastern part of the Sørkapp Basin comprises the deepest segment of the Paleozoic basin complex and coincides with a local gravity maximum (+50 mGal) as well as elevated velocities in the deep crust (Figure 7; Breivik et al., 2003, 2005). Accordingly, we interpret the Sørkapp Basin in the sense of Anell et al. (2014) as W-E striking half-graben that opens westward into the N-S to NNE-SSW striking Sørkapp Depression. The Sørkapp Basin extends eastward across BGR2015–106 accompanied by a positive gravity anomaly (Figure 6a). Its eastern limit, however, is difficult to determine. A seismic profile published by Høy and Lundschien (2011) indicates a Paleozoic graben south of the late Mesozoic/Cenozoic inverted Sentralbanken High in prolongation of the here identified eastern segment of the Sørkapp Basin. This graben is similarly delineated by a W-E oriented positive gravity anomaly (Figure 6) and may represent the further eastern prolongation of the Sørkapp Basin (Figure 6).
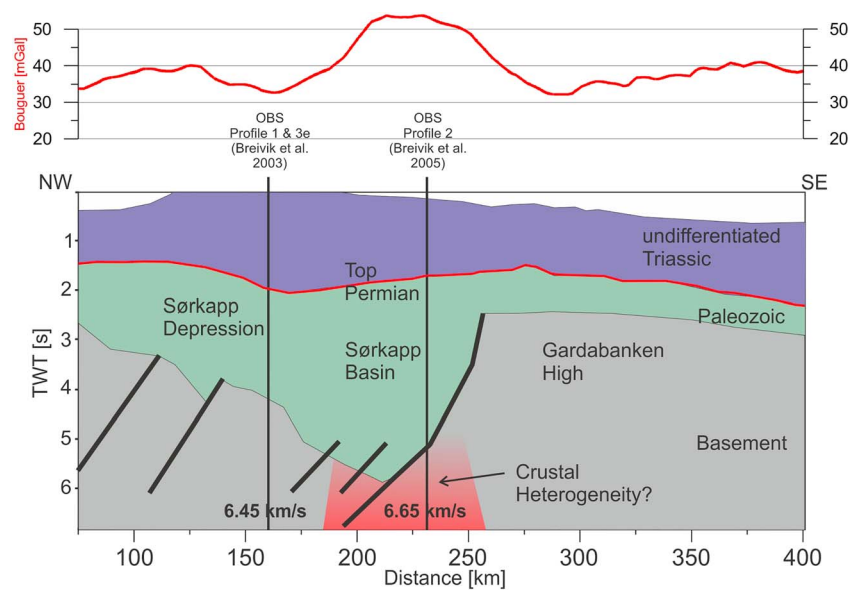
Figure 7. Simplified seismic profile from Glørstad-Clark et al. (2010) and intersection with OBS profiles from Breivik et al. (2003, 2005) and corresponding average basement velocity. See Figure 6 for location. Elevated velocities (6.65 km/s; Breivik et al., 2005) coincide with a gravity maximum below the Sørkapp Basin and are interpreted as deep crustal magmatic intrusions.

From the similar structural configuration and basin architecture, we suggest that both basins, the Olga Basin and the wider Sørkapp Basin, evolved as part of the same system in late Devonian/early Carboniferous.

6. Tectonic Affinity of the Olga-Sørkapp Region

6.1. Caledonian Terrane

Recent investigations on the Caledonian grain show that the strike of the Caledonian thrust and nappes rotates counterclockwise from a NE-SW trend onshore Norway to a NNW-SSE trend in the SW Barents Sea (Figure 1; Barrère et al., 2009, 2011; Gernigon et al., 2014; Gernigon & Brönner, 2012). Short-wavelength magnetic anomalies are assumed to delineate the Caledonian basement grain (Gernigon et al., 2014, 2018; Gernigon & Brönner, 2012). Following these magnetic anomalies from the SW Barents Sea, the Caledonian grain converges northward east of Bjørnøya and broadens again south of Svalbard, indicating a widening of the Caledonian collision zone in the north (Figure 6b). A wider Caledonian collision in the north is further supported by petrological, structural, and geochronological evidence from the Svalbard region (Gasser & Andresen, 2013; Johansson et al., 2005; Majka & Kośmińska, 2017; Mazur et al., 2009). Eastward increasing metamorphic gradients and severity of deformation (Johansson et al., 2005; Tebenkov et al., 2002) imply that the Caledonian suture is located east of Svalbard (Figure 6b; Barrère et al., 2009, 2011). However, by following the short-wavelength magnetic expression of the Caledonian nappes and thrust sheets (Barrère et al., 2009, 2011; Gernigon et al., 2014, 2018; Gernigon & Brönner, 2012), the corresponding Caledonian suture may run west of our study area (red lines in Figure 6).

A second NE-oriented Caledonian arm across the Olga and Sørkapp Basins (Figure 1) is questioned for a number of reasons. Given the here identified W-E trend for both, the Olga Basin and the Sørkapp Basin, the suggested NNE-SSW striking Caledonian trend would crosscut axis of the Olga Basin almost perpendicularly (Figure 1). The widespread accepted low-angle décollements underlying Caledonian collapse basins (Fossen & Hurich, 2005; Osmundsen & Andersen, 2001) would cut the Caledonian basal thrust zone at a high angle, making a relationship between the Caledonian structural grain and the two basins unlikely. In addition, both magnetic and gravity data (Figure 6) are not in favor of such a trend. Elevated deep crustal velocity anomalies, as detected by Aarseth et al. (2017) and Breivik et al. (2003, 2005), may reflect two separate deep crustal heterogeneities underlying Olga and Sørkapp Basins rather than the Caledonian grain.
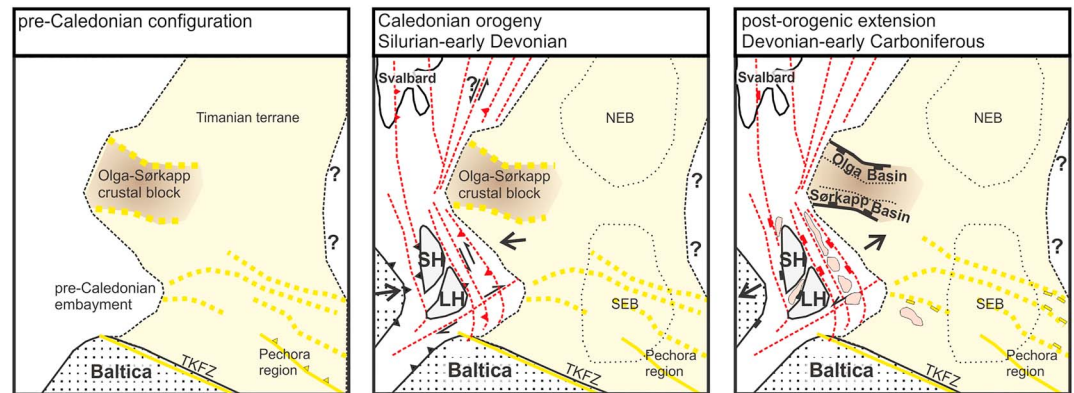
Figure 8. Conceptual sketch of the Paleozoic geological evolution of the Barents Sea (not to scale). (a) Different terranes accreted along NE Baltica during the Timanian orogeny including also the Olga-Sørkapp crustal block. (b) A westward exposed position of the Olga-Sørkapp crustal block would explain the counterclockwise rotation of Caledonian thrust sheets and nappes as interpreted in high-resolution magnetic data (Gernigon et al., 2014). Drawings of the SW Barents Sea are based on Gernigon et al. (2014). (c) Regional extension during late Devonian to early carboniferous reactivated old Timanian (yellow) and Caledonian (red) structures which possibly resulted in formation of the Olga and Sørkapp Basins as well as sedimentary basins in the SW Barents Sea (Gernigon et al., 2014) and the Pechora region (Ivanova et al., 2011). LH = Loppa High, NEB = NE Barents Sea Basin, SEB = SE Barents Sea Basin, SH = Stappen High, TKFZ = Trollfjorden-Komagelva Fault Zone.

6.2. Timanian Terrane

The Olga-Sørkapp region is located in prolongation of assumed NW-SE striking Timanian trends from the Pechora Basin and the SE Barents Sea (Dovzhikova et al., 2004; Gernigon et al., 2018; Roberts & Siedlecka, 2002; Shulgin et al., 2018). We suggest from similar magnetic and gravity patterns in both regions that Timanian accretion of Neoproterozoic fragments has occurred further west than previously assumed (Figure 6). A Timanian basement grain below the wider Olga Basin region would explain the general W-E orientation of structural elements including the deep crustal folds (Figures 3 and 4), the Paleozoic axis of the Olga and Sørkapp Basins, the W-E oriented potential field anomalies (Figure 6), and a W-E striking mild Moho uplift below the Olga Basin (Breivik et al., 2002).

In our view, the late Precambrian to Cambrian accretion of Neoproterozoic fragments and metamorphosed sedimentary, volcanic, and volcanoclastic rocks may have included also an Olga-Sørkapp crustal block (Figure 8a). If so, a western Timanian margin would be characterized by a westward exposed position of the Olga-Sørkapp crustal block and an embayment in the present-day SW Barents Sea. During the collision of Laurentia and Baltica in Silurian times the westward exposed Olga-Sørkapp crustal block may have caused the counterclockwise rotation of the Caledonian thrust sheets and nappes in the SW Barents Sea (Figure 8b; Barrère et al., 2009, 2011; Gernigon et al., 2014; Gernigon & Brönner, 2012).

Following the Caledonian compressive regime, a polyphasal rift evolution started on Laurussia and along its margins in the Paleozoic. A middle Devonian NE-SW oriented rifting occurred in the Pechora Basin along old Timanian structures. This extensional phase was at least partly accompanied by magmatism and reached the eastern Barents Sea in late Devonian-early Carboniferous (Ivanova et al., 2011; Nasuti et al., 2015; Petrov et al., 2008; Stoupakova et al., 2011). Possibly, this extensional episode reached also the central Barents Sea and reactivated deep Timanian structures resulting in the formation of the Olga and Sørkapp Basins (Figure 8c). The presence of old zones of weakness may have facilitated magmatism which would explain the basin-wide positive gravity and magnetic anomalies as well as the elevated velocities in the deep crust (Breivik et al., 2002, 2003, 2005). Additionally, it appears that this rifting phase coincides with the extensional collapse of the Caledonides and corresponding basin formation in the western Barents Sea and with late Devonian-early Carboniferous rifting on Svalbard (Baelum et al., 2012; Gernigon et al., 2014, 2018; Gernigon & Brönner, 2012). Later this extensional system was followed by the proto-Atlantic rifting phase in the western Barents Sea evident in the NE-SW striking graben, that is, the Nordkapp Basin, across the Kong-Karl Platform and below the Sentralbanken High (Faleide et al., 2010; Gernigon et al., 2018; NPD, 2017).

7. Conclusions

1. We use newly acquired multichannel reflection seismic data to assess the structural configuration of the Olga Basin region. The combined interpretation of seismic and potential field data shed new light onto the deep crustal structure of the NE Norwegian Barents Sea and allow a better understanding in particular of the Paleozoic evolution of the sedimentary basins.

2. Seismic stratigraphy can be tied with confidence to Permian, Triassic, and Cretaceous strata. Cretaceous deposits are only locally preserved in the Olga Basin and across the Kong Karl Platform related to widespread inversion tectonics in late Mesozoic-Cenozoic times. Jurassic strata are highly condensed if present at all. During Triassic regional subsidence, the Barents Sea was filled with clastic sediments from the Uralian orogen resulting in the formation of prominent regional superimposed early and middle Triassic clinoforms. These Triassic clinoforms downlap on a strong regional reflector characterizing the deposition of spiculites in the late Permian. Below, a second regional reflector is associated with the mid-Carboniferous transgression and a lithological change from sandstones and shales to silicified deposits, carbonates, and evaporites. Notably, we find no indications for Carboniferous-Permian rifting phases within the Olga Basin as widely observed in the southern and western Barents Sea. Wedge-shaped syn-extensional sediments of unknown age illustrate the initial subsidence phase of the Olga Basin which evolved as half-graben in response to mild extension. These deepest sediments are bound by a major Paleozoic normal fault at the northern rim of the basin. The absence of compressional deformation implies a post-Caledonian onset of subsidence.

3. Deep parallel reflections below the mid-Carboniferous horizon at depths of 3–4 s TWT on profile BGR2015–106 (Figure 4) indicate a so far unknown half-graben bounded by a major normal fault in the south. The combined analysis of seismic reflection and potential field data suggest that this basin represents the eastern extension of the Sørkapp Basin running parallel to the Olga Basin. Both basins are delineated by local magnetic and gravimetric maxima implying deep crustal heterogeneities.

4. Deep undulating high-amplitude reflections at depths of 3.5–6 s (TWT) with a wavelength of 50 km may indicate the remnants of an orogeny (Figures 2 and 4). The topography of these high-amplitude reflections coincides with a W-E striking local magnetic maximum.

5. The Olga-Sørkapp basin system strikes almost perpendicular to the proposed Caledonian trends of the NW Barents Sea. A commonly proposed Caledonian low-angle décollement resulting in basin formation would cut the Caledonian basal thrust zone at a high angle, making a relationship between the Caledonian structural grain and the Olga Basin highly unlikely.

6. The orientation of the Olga and Sørkapp basin axis is situated in the prolongation of Timanian trends from the SE Barents Sea and the Pechora Basin. This suggests that the Olga Basin region is underlain by Timanian basement. A salient pre-Caledonian crustal block in the central Barents Sea additionally explains the NNW rotation of Caledonian nappes and thrust sheets in the SW Barents Sea.

7. We suggest that late Devonian-early Carboniferous NE-SW extension, as proposed to explain deep Paleozoic basins of the Timan-Pechora region, reached as far as to the Olga-Sørkapp region. The deeper Timanian grain is proposed to have influenced the final W-E configuration and resulted likely in the formation of the Olga and Sørkapp Basins.

References

Aarseth, I., Mjelde, R., Breivik, A. J., Minakov, A., Faleide, J. I., Flueh, E., & Huismans, R. S. (2017). Crustal structure and evolution of the Arctic Caledonides: Results from controlled-source seismology. *Tectonophysics*, *718*, 9–24. https://doi.org/10.1016/j.tecto.2017.04.022

Andersen, O. B., Knudsen, P., Kenyon, S., & Holmes, S. (2014). Global and arctic marine gravity field from recent satellite altimetry (DTU13). In *76th European Association of Geoscientists and Engineers Conference and Exhibition* 2014: *Experience the Energy - Incorporating SPE EUROPEC* 2014 (pp. 3049–3053). Retrieved from https://www.scopus.com/inward/record.uri?eid=2-s2.0-84907415940&partnerID=40&md5=9d94b62a0ae451109ab76d28c55095f0

Anell, I., Braathen, A., & Olaussen, S. (2014). Regional constraints of the Sørkapp Basin: A carboniferous relic or a cretaceous depression? *Marine and Petroleum Geology*, *54*, 123–138. https://doi.org/10.1016/j.marpetgeo.2014.02.023

Anell, I., Braathen, A., Olaussen, S., & Osmundsen, P. T. (2013). Evidence of faulting contradicts a quiescent northern Barents shelf during the Triassic. *First Break*, *31*(1978), 67–76. https://doi.org/10.3997/1365-2397.2013017

Anell, I., Faleide, J. I., & Braathen, A. (2016). Regional tectono-sedimentary development of the highs and basins of the northwestern Barents shelf. *Norwegian Journal of Geology*, *96*(1), 27–41. https://doi.org/10.17850/njg96-1-04

Antonsen, P., Elverhoi, A., Dypvik, H., & Solheim, A. (1991). Shallow bedrock geology of the Olga Basin area, northwestern Barents Sea. *American Association of Petroleum Geologists Bulletin*, *75*(7), 1178–1194.

Baelum, K., Braathen, A., Bælum, K., & Braathen, A. (2012). Along-strike changes in fault array and rift basin geometry of the carboniferous Billefjorden trough, Svalbard, Norway. *Tectonophysics*, *546-547*, 38–55. https://doi.org/10.1016/j.tecto.2012.04.009

Baig, I., Faleide, J. I., Jahren, J., & Mondol, N. H. (2016). Cenozoic exhumation on the southwestern Barents shelf: Estimates and uncertainties constrained from compaction and thermal maturity analyses. *Marine and Petroleum Geology*, *73*, 105–130. https://doi.org/10.1016/j.marpetgeo.2016.02.024

Barrère, C., Ebbing, J., & Gernigon, L. (2009). Offshore prolongation of Caledonian structures and basement characterisation in the western Barents Sea from geophysical modelling. *Tectonophysics*, *470*(1–2), 71–88. https://doi.org/10.1016/j.tecto.2008.07.012

Barrère, C., Ebbing, J., & Gernigon, L. (2011). 3-D density and magnetic crustal characterization of the southwestern Barents shelf: Implications for the offshore prolongation of the Norwegian Caledonides. *Geophysical Journal International*, *184*(3), 1147–1166. https://doi.org/10.1111/j.1365-246X.2010.04888.x

Blaich, O. A., Tsikalas, F., & Faleide, J. I. (2017). New insights into the tectono-stratigraphic evolution of the southern Stappen high and its transition to Bjørnøya Basin, SW Barents Sea. *Marine and Petroleum Geology*, *85*, 89–105. https://doi.org/10.1016/j.marpetgeo.2017.04.015

Blystad, P., Brekke, H., Færseth, R. B., Larsen, B. T., Skogseid, J., & Tærudbakken, B. (1995). Structural elements of the Norwegian continental shelf. Part II. The Norwegian Sea Region. *NPD Bulletin No. 8*.

Breivik, A. J., Gudlaugsson, S. T., & Faleide, J. I. (1995). Ottar Basin, SW Barents Sea: A major upper Palaeozoic rift basin containing large volumes of deeply buried salt. *Basin Research*, *7*(4), 299–312. https://doi.org/10.1111/j.1365-2117.1995.tb00119.x

Breivik, A. J., Mjelde, R., Grogan, P., Shimamura, H., Murai, Y., & Nishimura, Y. (2003). Crustal structure and transform margin development south of Svalbard based on ocean bottom seismometer data. *Tectonophysics*, *369*(1–2), 37–70. https://doi.org/10.1016/S0040-1951(03)00131-8

Breivik, A. J., Mjelde, R., Grogan, P., Shimamura, H., Murai, Y., & Nishimura, Y. (2005). Caledonide development offshore-onshore Svalbard based on ocean bottom seismometer, conventional seismic, and potential field data. *Tectonophysics*, *401*(1–2), 79–117. https://doi.org/10.1016/j.tecto.2005.03.009

Breivik, A. J., Mjelde, R., Grogan, P., Shimamura, H., Murai, Y., Nishimura, Y., & Kuwano, A. (2002). A possible Caledonide arm through the Barents Sea imaged by OBS data. *Tectonophysics*, *355*(1–4), 67–97. https://doi.org/10.1016/S0040-1951(02)00135-X

Clark, S. A., Glorstad-Clark, E., Faleide, J. I., Schmid, D., Hartz, E. H., & Fjeldskaar, W. (2014). Southwest Barents Sea rift basin evolution: Comparing results from backstripping and time-forward modelling. *Basin Research*, *26*(4), 550–566. https://doi.org/10.1111/bre.12039

Corfu, F., Polteau, S., Planke, S., Faleide, J. I., Svensen, H., Zayoncheck, A., & Stolbov, N. (2013). U-Pb geochronology of cretaceous magmatism on Svalbard and Franz Josef Land, Barents Sea large igneous province. *Geological Magazine*, *150*(06), 1127–1135. https://doi.org/10.1017/S0016756813000162

Dallmann, W. K., Blomeier, D., & Elvevold, S. (2015). *Geoscience Atlas of Svalbard. Norsk Polarinstitutt Årbok 148*. Tromsø, Norway. https://doi.org/10.1017/S0016756800196311

Dimakis, P., Braathen, B. I., Faleide, J. I., Elverhøi, A., & Gudlaugsson, S. T. (1998). Cenozoic erosion and the preglacial uplift of the Svalbard–Barents Sea region. *Tectonophysics*, *300*(1–4), 311–327. https://doi.org/10.1016/S0040-1951(98)00245-5

Doré, A. G., Lundin, E. R., Fichler, C., & Olesen, O. (1997). Patterns of basement structure and reactivation along the NE Atlantic margin. *Journal of the Geological Society*, *154*(1), 85–92. https://doi.org/10.1144/gsjgs.154.1.0085

Dovzhikova, E., Pease, V., & Remizov, D. (2004). Neoproterozoic island are magmatism beneath the Pechora Basin, NW Russia. *GFF*, *126*(4), 353–362. https://doi.org/10.1080/11035890401264353

Eide, C. H., Klausen, T. G., Katkov, D., Suslova, A. A., & Helland-Hansen, W. (2017). Linking an Early Triassic delta to antecedent topography: Source-to-sink study of the southwestern Barents Sea margin. *GSA Bulletin*. https://doi.org/10.1130/B31639.1

Eiken, O. (1994). Seismic atlas of Western Svalbard: A selection of regional\rseismic transects. *Meddelelser, Nr. 130, Norsk Polarinstitutt, Oslo*. Retrieved from https://brage.bibsys.no/xmlui/handle/11250/2396881

Estrada, S., Tessensohn, F., & Sonntag, B. L. (2018). A Timanian island-arc fragment in North Greenland: The Midtkap igneous suite. *Journal of Geodynamics*, *118*, 140–153. https://doi.org/10.1016/j.jog.2018.01.015

Faleide, J. I., Bjørnlykke, K., & Gabrielsen, R. H. (2010). Geology of the Norwegian continental shelf. In *Petroleum Geoscience: From Sedimentary Environments to Rock Physics* (pp. 467–499). Berlin Heidelberg: Springer. https://doi.org/10.1007/978-3-642-02332-3

Faleide, J. I., Gudlaugsson, S. T., & Jacquart, G. (1984). Evolution of the western Barents Sea. *Marine and Petroleum Geology*, *1*(2), 123–150. https://doi.org/10.1016/0264-8172(84)90082-5

Faleide, J. I., Pease, V., Curtis, M., Klitzke, P., Minakov, A., Scheck-Wenderoth, M., et al. (2018). Tectonic implications of the lithospheric structure across the Barents and Kara shelves. *Geological Society, London, Special Publications*, *460*(1), 285–314. https://doi.org/10.1144/SP460.18

Faleide, J. I., Vågnes, E., & Gudlaugsson, S. T. (1993). Late Mesozoic-Cenozoic evolution of the South-Western Barents Sea in a regional rift-shear tectonic setting. *Marine and Petroleum Geology*, *10*(3), 186–214. https://doi.org/10.1016/0264-8172(93)90104-Z

Fleming, E. J., Flowerdew, M. J., Smyth, H. R., Scott, R. A., Morton, A. C., Omma, J. E., et al. (2016). Provenance of Triassic sandstones on the southwest Barents shelf and the implication for sediment dispersal patterns in northwest Pangaea. *Marine and Petroleum Geology*, *78*, 516–535. https://doi.org/10.1016/j.marpetgeo.2016.10.005

Fossen, H., & Hurich, C. a. (2005). The Hardangerfjord shear zone in SW Norway and the North Sea: A large-scale low-angle shear zone in the Caledonian crust. *Journal of the Geological Society*, *162*(4), 675–687. https://doi.org/10.1144/0016-764904-136

Franke, D., Reichert, C., Damm, V., & Piepjohn, K. (2008). The south Anyui suture, northeast arctic Russia, revealed by offshore seismic data. *Norsk Geologisk Tidsskrift*, *88*(4), 189–200.

Gabrielsen, R. H., Færseth, R. B., Jensen, L. N., Kalheim, J. E., & Riis, F. (1990). Structural elements of the Norwegian continental shelf, part I: The Barents Sea region. *Norwegian Petroleum Directorate. Bulletin*, *6*, 1–47. Retrieved from http://npd.no/engelsk/infoserv/publ/NPD_BulletinNo4.pdf

Gaina, C., Werner, S. C., Saltus, R., & Maus, S. (2011). Circum-Arctic mapping project: New magnetic and gravity anomaly maps of the Arctic. *Geological Society, London, Memoirs*, *35*(1), 39–48. https://doi.org/10.1144/M35.3

Gasser, D., & Andresen, A. (2013). Caledonian terrane amalgamation of Svalbard: Detrital zircon provenance of Mesoproterozoic to carboniferous strata from Oscar II land, western Spitsbergen. *Geological Magazine*, *150*(06), 1103–1126. https://doi.org/10.1017/S0016756813000174

Gee, D. G., Bogolepova, O. K., & Lorenz, H. (2006). The Timanide, Caledonide and Uralide orogens in the Eurasian high Arctic, and relationships to the palaeo-continents Laurentia, Baltica and Siberia. *Geological Society, London, Memoirs*, *32*(1), 507–520. https://doi.org/10.1144/GSL.MEM.2006.032.01.31

Gee, D. G., Fossen, H., Henriksen, N., & Higgins, A. K. (2008). From the early Paleozoic platforms of Baltica and Laurentia to the Caledonide orogen of Scandinavia and Greenland. *Episodes*, *31*(1), 44–51.

Gee, D. G., & Pease, V. (2004). The Neoproterozoic Timanide Orogen of eastern Baltica: Introduction. *Geological Society, London, Memoirs*, *30*(1), 1–3. https://doi.org/10.1144/GSL.MEM.2004.030.01.01

Gérard, J., & Buhrig, C. (1990). Seismic facies of the Permian section of the Barents shelf: Analysis and interpretation. *Marine and Petroleum Geology*, *7*(3), 234–252. https://doi.org/10.1016/0264-8172(90)90002-X

Gernigon, L., & Brönner, M. (2012). Late Palaeozoic architecture and evolution of the southwestern Barents Sea: Insights from a new generation of aeromagnetic data. *Journal of the Geological Society*, *169*(4), 449–459. https://doi.org/10.1144/0016-76492011-131

Gernigon, L., Brönner, M., Dumais, M. A., Gradmann, S., Grønlie, A., Nasuti, A., & Roberts, D. (2018). Basement inheritance and salt structures in the SE Barents Sea: Insights from new potential field data. *Journal of Geodynamics*, *119*, 82–106. https://doi.org/10.1016/j.jog.2018.03.008

Gernigon, L., Brönner, M., Fichler, C., Løvås, L., Marello, L., & Olesen, O. (2011). Magnetic expression of salt diapir-related structures in the Nordkapp Basin, western Barents Sea. *Geology*, *39*(2), 135–138. https://doi.org/10.1130/G31431.1

Gernigon, L., Brönner, M., Roberts, D., Olesen, O., Nasuti, A., & Yamasaki, T. (2014). Crustal and basin evolution of the southwestern Barents Sea: From Caledonian orogeny to continental breakup. *Tectonics*, *33*, 347–373. https://doi.org/10.1002/2013TC003439

Glørstad-Clark, E., Birkeland, E. P., Nystuen, J. P., Faleide, J. I., & Midtkandal, I. (2011). Triassic platform-margin deltas in the western Barents Sea. *Marine and Petroleum Geology*, *28*(7), 1294–1314. https://doi.org/10.1016/j.marpetgeo.2011.03.006

Glørstad-Clark, E., Faleide, J. I., Lundschien, B. A., & Nystuen, J. P. (2010). Triassic seismic sequence stratigraphy and paleogeography of the western Barents Sea area. *Marine and Petroleum Geology*, *27*(7), 1448–1475. https://doi.org/10.1016/j.marpetgeo.2010.02.008

Green, P. F., & Duddy, I. R. (2010). Synchronous exhumation events around the Arctic including examples from Barents Sea and Alaska north slope. In B. A. Vining, & S. C. Pickering (Eds.), *Petroleum Geology: From Mature Basins to New FrontiersProceedings of the 7th Petroleum Geology Conference. Petroleum Geology Conference Series* (Vol. 7, pp. 633–644). London: Geological Society. https://doi.org/10.1144/0070633

Grogan, P., Nyberg, K., Fotland, B., Myklebust, R., Dahlgren, S., & Riis, F. (2000). Cretaceous magmatism south and east of Svalbard: Evidence from seismic reflection and magnetic data. *Polarforschung*, *68*(1–3), 25–34.

Grundvåg, S.-A., Marin, D., Kairanov, B., Śliwińska, K. K., Nøhr-Hansen, H., Jelby, M. E., et al. (2017). The lower cretaceous succession of the northwestern Barents shelf: Onshore and offshore correlations. *Marine and Petroleum Geology*, *86*, 834–857. https://doi.org/10.1016/j.marpetgeo.2017.06.036

Gudlaugsson, S. T., Faleide, J. I., Johansen, S. E., & Breivik, A. J. (1998). Late Palaeozoic structural development of the South-Western Barents Sea. *Marine and Petroleum Geology*, *15*(1), 73–102. https://doi.org/10.1016/S0264-8172(97)00048-2

Harland, W. B., & Wright, N. J. R. (1979). Alternative hypothesis for the pre-carboniferous evolution of Svalbard. *Norsk Polarinstitutt Tiddskrifter*, *167*, 89–117.

Henriksen, E., Bjørnseth, H. M., Hals, T. K., Heide, T., Kiryukhina, T., Kløvjan, O. S., et al. (2011). Chapter 17 uplift and erosion of the greater Barents Sea: Impact on prospectivity and petroleum systems. *Geological Society, London, Memoirs*, *35*(1), 271–281. https://doi.org/10.1144/M35.17

Henriksen, E., Ryseth, A. E., Larssen, G. B., Heide, T., Rønning, K., Sollid, K., & Stoupakova, A. V. (2011). Chapter 10 Tectonostratigraphy of the greater Barents Sea: Implications for petroleum systems. *Geological Society, London, Memoirs*, *35*(1), 163–195. https://doi.org/10.1144/M35.10

Høy, T., & Lundschien, B. A. (2011). Chapter 15 Triassic deltaic sequences in the northern Barents Sea. *Geological Society, London, Memoirs*, *35*(1), 249–260. https://doi.org/10.1144/M35.15

Ivanova, N. M., Sakulina, T. S., Belyaev, I. V., Matveev, Y. I., & Roslov, Y. V. (2011). Chapter 12 depth model of the Barents and Kara Seas according to geophysical surveys results. *Geological Society, London, Memoirs*, *35*(1), 209–221. https://doi.org/10.1144/M35.12

Johansson, Å., Gee, D. G., Larionov, A. N., Ohta, Y., & Tebenkov, A. M. (2005). Grenvillian and Caledonian evolution of eastern Svalbard— A tale of two orogenies. *Terra Nova*, *17*(4), 317–325. https://doi.org/10.1111/j.1365-3121.2005.00616.x

Klausen, T. G. (2013). Does evidence of faulting contradict a quiescent northern Barents shelf during the Triassic? *First Break*, *31*(1978), 67–76. Retrieved from http://fb.eage.org/publication/content?id=69638

Klitzke, P., Faleide, J. I., Scheck-Wenderoth, M., & Sippel, J. (2015). A lithosphere-scale structural model of the Barents Sea and Kara Sea region. *Solid Earth*, *6*(1), 153–172. https://doi.org/10.5194/se-6-153-2015

Klitzke, P., Sippel, J., Faleide, J. I., & Scheck-Wenderoth, M. (2016). A 3D gravity and thermal model for the Barents Sea and Kara Sea. *Tectonophysics*, *684*, 131–147. https://doi.org/10.1016/j.tecto.2016.04.033

Knudsen, C., Hopper, J. R., Bierman, P. R., Bjerager, M., Funck, T., Green, P. F., et al. (2017). Samples from the Lomonosov ridge place new constraints on the geological evolution of the Arctic Ocean. *Geological Society, London, Special Publications*, *460*(1), 397. https://doi.org/10.1144/SP460.17–418.

Koehl, J.-B. P., Bergh, S. G., Henningsen, T., & Faleide, J. I. (2018). Middle to late Devonian-carboniferous collapse basins on the Finnmark platform and in the southwesternmost Nordkapp basin, SW Barents Sea. *Solid Earth*, *9*(2), 341–372. https://doi.org/10.5194/se-9-341-2018

Larssen, G. B., Elvebakk, G., Henriksen, L. B., Nilsson, I., Samuelsberg, T. J., Stemmerik, L., & Worsley, D. (2002). Upper Palaeozoic lithostratigraphy of the southern Norwegian Barents Sea. *Norwegian Petroleum Directorate. Bulletin*, *9*, 76.

Lundschien, B. A., Høy, T., & Mørk, A. (2014). Triassic hydrocarbon potential in the northern Barents Sea; integrating Svalbard and stratigraphic core data. *Norwegian Petroleum Directorate. Bulletin*, *11*(11), 3–20.

Maher, H. D. Jr. (2001). Manifestations of the Cretaceous high Arctic Large Igneous Province in Svalbard. *The Journal of Geology*, *109*(1), 91–104. https://doi.org/10.1086/317960

Majka, J., & Kośmińska, K. (2017). Magmatic and metamorphic events recorded within the southwestern basement province of Svalbard. *Arktos*, *3*(1), 5. https://doi.org/10.1007/s41063-017-0034-7

Manby, G., & Lyberis, N. (1992). Tectonic evolution of the Devonian Basin of northern Svalbard. *Norsk Geologisk Tidsskrift*, *72*(1), 7–19.

Marello, L., Ebbing, J., & Gernigon, L. (2013). Basement inhomogeneities and crustal setting in the Barents Sea from a combined 3D gravity and magnetic model. *Geophysical Journal International*, *193*(2), 557–584. https://doi.org/10.1093/gji/ggt018

Mazur, S., Czerny, J., Majka, J., Manecki, M., Holm, D., Smyrak, A., & Wypych, A. (2009). A strike-slip terrane boundary in wedel Jarlsberg land, Svalbard, and its bearing on correlations of SW Spitsbergen with the Pearya terrane and Timanide belt. *Journal of the Geological Society*, *166*(3), 529–544. https://doi.org/10.1144/0016-76492008-106

Minakov, A., Mjelde, R., Faleide, J. I., Flueh, E. R., Dannowski, A., & Keers, H. (2012). Mafic intrusions east of Svalbard imaged by active-source seismic tomography. *Tectonophysics*, *518-521*, 106–118. https://doi.org/10.1016/j.tecto.2011.11.015

Minakov, A., Yarushina, V., Faleide, J. I., Krupnova, N., Sakoulina, T., Dergunov, N., & Glebovsky, V. (2017). Dyke emplacement and crustal structure within a continental large igneous province, northern Barents Sea. *Geological Society, London, Special Publications*, *460*(1), 371. https://doi.org/10.1144/SP460.4–395

Nasuti, A., Roberts, D., & Gernigon, L. (2015). Multiphase mafic dykes in the Caledonides of northern Finnmark revealed by a new high-resolution aeromagnetic dataset. *Norwegian Journal of Geology Nr*, *3*(3), 285–297. https://doi.org/10.17850/njg95-3-02

Nilsen, K. T., Vendeville, B. C., & Johansen, J.-T. (1995). Influence of regional tectonics an Halokinesis in the Nordkapp Basin, Barents Sea. *Salt Tectonics: A Global Prespective: AAPG Memoir*, *65*, 413–436.

NPD. (2017). Geological assessment of petroleum resources in eastern parts of Barents Sea north 2017. Retrieved from http://www.npd.no/en/Publications/Reports/Geological-assessment-of-petroleum-resources---Barents-Sea-north-2017/

Osmundsen, P. T., & Andersen, T. B. (2001). The middle Devonian basins of western Norway: Sedimentary response to large-scale transtensional tectonics? *Tectonophysics*, *332*(1–2), 51–68. https://doi.org/10.1016/S0040-1951(00)00249-3

Osmundsen, P. T., Braathen, A., Rød, R. S., & Hynne, I. B. (2014). Styles of normal faulting and fault-controlled sedimentation in the Triassic deposits of eastern Svalbard. *Norwegian Petroleum Directorate. Bulletin*, *11*(11), 61–79.

Pease, V. (2011). Chapter 20 Eurasian orogens and Arctic tectonics: An overview. *Geological Society, London, Memoirs*, *35*(1), 311–324. https://doi.org/10.1144/M35.20

Perez-Garcia, C., Safronova, P. A., Mienert, J., Berndt, C., & Andreassen, K. (2013). Extensional rise and fall of a salt diapir in the Sørvestsnaget Basin, SW Barents Sea. *Marine and Petroleum Geology*, *46*, 129–143. https://doi.org/10.1016/j.marpetgeo.2013.05.010

Petrov, O. V., Sobolev, N. N., Koren, T. N., Vasiliev, V. E., Petrov, E. O., Larssen, G. B., & Smelror, M. (2008). Palaeozoic and early Mesozoic evolution of the east Barents and Kara Seas sedimentary basins. *Norsk Geologisk Tidsskrift*, *88*(4), 227–234. Retrieved from http://geologi.imaker.no/data/f/0/19/83/2_2401_0/NJG_Petrov_et_al_4_2008_screen.pdf

Polteau, S., Hendriks, B. W. H., Planke, S., Ganerød, M., Corfu, F., Faleide, J. I., Midtkandal, I., et al. (2015). The Early Cretaceous Barents Sea sill complex: Distribution, ^{40}Ar/^{39}Ar geochronology, and implications for carbon gas formation. *Palaeogeography, Palaeoclimatology, Palaeoecology*, *441*, 83–95. https://doi.org/10.1016/j.palaeo.2015.07.007

Pózer Bue, E., & Andresen, A. (2014). Constraining depositional models in the Barents Sea region using detrital zircon U–Pb data from Mesozoic sediments in Svalbard. *Geological Society, London, Special Publications*, *386*(1), 261–279. https://doi.org/10.1144/SP386.14

Puchkov, V. N. (2009). The evolution of the Uralian orogen. *Geological Society of London, Special Publications*, *327*(1), 161–195. https://doi.org/10.1144/SP327.9

Rasmussen, E., & Fjeldskaar, W. (1996). Quantification of the Pliocene-Pleistocene erosion of the Barents Sea from present-day bathymetry. *Global and Planetary Change*, *12*(1-4), 119–133. https://doi.org/10.1016/0921-8181(95)00015-1

Riis, F., Lundschien, B. A., Høy, T., Mørk, A., & Mørk, M. B. E. (2008). Evolution of the Triassic shelf in the northern Barents Sea region. *Polar Research*, *27*(3), 318–338. https://doi.org/10.1111/j.1751-8369.2008.00086.x

Ritzmann, O., & Faleide, J. I. (2007). Caledonian basement of the western Barents Sea. *Tectonics*, *26*, TC5014. https://doi.org/10.1029/2006TC002059

Ritzmann, O., & Faleide, J. I. (2009). The crust and mantle lithosphere in the Barents Sea/Kara Sea region. *Tectonophysics*, *470*(1–2), 89–104. https://doi.org/10.1016/j.tecto.2008.06.018

Roberts, D., & Siedlecka, A. (2002). Timanian orogenic deformation along the northeastern margin of Baltica, Northwest Russia and Northeast Norway, and Avalonian-Cadomian connections. *Tectonophysics*, *352*(1–2), 169–184. https://doi.org/10.1016/S0040-1951(02)00195-6

Serck, C. S., Faleide, J. I., Braathen, A., Kjølhamar, B., & Escalona, A. (2017). Jurassic to early cretaceous basin configuration(s) in the Fingerdjupet subbasin, SW Barents Sea. *Marine and Petroleum Geology*, *86*, 874–891. https://doi.org/10.1016/j.marpetgeo.2017.06.044

Shulgin, A., Mjelde, R., Faleide, J. I., Høy, T., Flueh, E., & Thybo, H. (2018). The crustal structure in the transition zone between the western and eastern Barents Sea. *Geophysical Journal International*, *214*(1), 315–330. https://doi.org/10.1093/gji/ggy139

Smelror, M., Petrov, O. V., Larssen, G. B., & Werner, S. (2009). In M. Smelror, O. Petrov, G. Larssen, & S. Werner (Eds.), *Geological History of the Barents SeaNorges Geol. undersøkelse* (). Trondheim, Norway: Geological Survey of Norway. Retrieved from http://www.ngu.no/upload/Publikasjoner/B?ker/Brosjyre-ATLAS-Barents.pdf

Sobolev, P. (2012). Cenozoic uplift and erosion of the eastern Barents Sea—Constraints from offshore well data and the implication for petroleum system modelling. *Zeitschrift der Deutschen Gesellschaft für Geowissenschaften*, *163*(3), 309–324. https://doi.org/10.1127/1860-1804/2012/0163-0323

Stadtler, C., Fichler, C., Hokstad, K., Myrlund, E. A., Wienecke, S., & Fotland, B. (2014). Improved salt imaging in a basin context by high resolution potential field data: Nordkapp Basin, Barents Sea. *Geophysical Prospecting*, *62*(3), 615–630. https://doi.org/10.1111/1365-2478.12101

Stoupakova, A. V., Henriksen, E., Burlin, Y. K., Larsen, G. B., Milne, J. K., Kiryukhina, T. A., Golynchik, P. O., et al. (2011). Chapter 21 the geological evolution and hydrocarbon potential of the Barents and Kara shelves. *Geological Society, London, Memoirs*, *35*(1), 325–344. https://doi.org/10.1144/M35.21

Tebenkov, A. M., Sandelin, S., Gee, D. G., & Johansson, Å. (2002). Caledonian migmatization in central Nordaustlandet, Svalbard. *Norsk Geologisk Tidsskrift*, *82*(2), 15–28.

Van Koeverden, J. H., Karlsen, D. A., Schwark, L., Chpitsglouz, A., & Backer-Owe, K. (2010). Oil-prone lower Carboniferous coals in the Norwegian Barents Sea: Implications for a Palaeozoic petroleum system. *Journal of Petroleum Geology*, *33*(2), 155–181. https://doi.org/10.1111/j.1747-5457.2010.00471.x

Worsley, D. (2008). The post-Caledonian development of Svalbard and the western Barents Sea. *Polar Research*, *27*(3), 298–317. https://doi.org/10.1111/j.1751-8369.2008.00085.x

Worsley, D., Agdestein, T., Gjelberg, J. G., Kirkemo, K., Mørk, A., Nilsson, I., Olaussen, S., et al. (2001). The geological evolution of Bjørnøya, Arctic Norway: Implications for the Barents shelf. *Norsk Geologisk Tidsskrift*, *81*(3), 195–234.

Zattin, M., Andreucci, B., de Toffoli, B., Grigo, D., & Tsikalas, F. (2016). Thermochronological constraints to late Cenozoic exhumation of the Barents Sea shelf. *Marine and Petroleum Geology*, *73*, 97–104. https://doi.org/10.1016/j.marpetgeo.2016.03.004